Advances in Concrete Construction, *Vol. 17, No. 4 (2024) 233-243*
https://doi.org/10.12989/acc.2024.17.4.233

Stress-strain response on the confined normal and high-strength concrete cylinders containing steel fiber under compression

Purwanto [1a], Antonius*[2] and Lisa Fitriyana [2b]

[1] *Universitas Semarang, Department of Civil Engineering, Semarang, Indonesia*
[2] *Universitas Islam Sultan Agung, Department of Civil Engineering, Semarang, Indonesia*

(*Received June 5, 2023, Revised July 14, 2024, Accepted August 27, 2024*)

Abstract. The behavior of confined steel fiber-reinforced concrete (including confinement models) with compressive strengths ranging from normal to high strength is still rarely studied. This paper presents the results of an investigation of fifteen confined concrete cylinders containing steel fiber. The design parameters evaluated in the experiment included concrete compressive strength (covers normal to high strength), volume fraction of steel fiber and hoop spacing. The main objective of this study was to evaluate the behavior of confined steel fiber concrete by reviewing several design parameters, such as concrete strength (normal to high strength). It is then developed to be an analytical stress-strain expression for confined steel fiber concrete. The experimental program was carried out by making cylindrical specimens with a diameter of 100 mm and a height of 200 mm. The cylindrical test object is compressed in a monotonic uniaxial loading. Experimental results have shown steel fiber in concrete has an important role in increasing the compressive strength and strain of cylindrical concrete without steel fiber. In addition, the value of strength enhancement of confined concrete (K) along with increasing fiber fraction volume; which applies to normal to high-strength concrete. The value of K also increases if the compressive strength of the concrete tends to decrease and the spacing of the hoops is closer. The comparison of stress-strain behavior between the confined steel fiber concrete proposed by other researchers and the experimental results in general significantly different in post-peak response. The statistical analysis indicates that the value of Coefficient of Variation for the confinement model by Campione is the closest compared to other existing confinement models in predicting the values of K and Toughness Index. Furthermore, the analytic stress-strain expression of confined steel fiber concrete was developed by adopting and modifying several equations from the present models. The proposed analytical expression is then verified with the experimental results. The results of the verification show that the stress-strain behavior of confined steel fiber concrete is relatively close.

Keywords: analytical expression; concrete strength; hoop; steel fiber; strength enhancement; toughness; volume fraction

1. Introduction

Fiber concrete one of the most desired materials for civil building structures today. This is due to the higher strength, better ductility, and abrasive resistance if normal concrete contains fiber in a certain volume fraction (Al-Tikrite and Hadi 2018, Jang and Yun 2018, Lu *et al*. 2018, Usman *et al*. 2020, Mansouri *et al*. 2020). The bond strength between steel fiber concrete and steel reinforcement is moreover, known to be better than the strength of normal concrete (García-Taengua *et al*. 2014). On the other hand, the results of an investigation conducted by Rabi *et al*. (2020) showed that stainless steel reinforcement has a lower adhesive strength to plain concrete compared to the adhesive strength between steel reinforcement and plain concrete. Due to the superior strength and ductility properties of fiber concrete, as mentioned above, steel fiber concrete installed with transverse reinforcement as confining reinforcement also has absolutely good ductility (Aoude *et al*. 2014, Antonius 2015, Amariansah and Karlinasari 2019). Steel-fiber concrete's flexural capacity and ductility in the beam structure, including the shear capacity, are equally higher than the capacity in normal concrete beams (Han *et al*. 2015, Sivakamasundari *et al*. 2017, Gomes *et al*. 2018).

Since it has both excellent performance and prospects for use in earthquake-resistant structures, the behavior of steel fiber concrete continues to be explored more thoroughly, as shown by its strength at high temperatures. The investigations included mechanical behavior, bending, shear, and confinement behavior of steel-fiber concrete at high temperatures (Zaidi *et al*. 2016, Antonius *et al*. 2019, 2020, Purwanto *et al*. 2021). Although many research results have been on steel fiber concrete, the design equations produced are still unregulated in the current standards (SNI 2847, ACI 318).

Combining steel fiber with concrete confined by transverse reinforcement will be one of the main choices in earthquake-resistant building structures. To a greater extent, this combination is very effective in significantly increasing the ductility of high-strength concrete columns in the design of earthquake-resistant structures. Meanwhile, the analytical expression of confined steel-fiber concrete is needed to

*Corresponding author, Ph.D., Professor,
E-mail: antonius@unissula.ac.id
[a] Lecturer, Ph.D., E-mail: purwanto_sipilusm@yahoo.com
[b] Lecturer, E-mail: lisa.fitriyana@unissula.ac.id

ISSN: 2287-5301 (Print), 2287-531X (Online)

design the confining reinforcement in the column structure to provide certainty of safety. The existing models of confinement of steel fiber concrete significantly differ, especially in predicting peak stress and post-peak behavior of stress-strain curves (Aoude *et al*. 2014, Antonius 2015, Cholida *et al*. 2022). Thus, it is necessary to develop the analytical expression of confined normal and high-strength concrete containing steel fiber, as carried out in this study. This study aimed to investigate the effect of steel fiber and some design parameters of the confining reinforcement on the behavior of the strength and ductility of confined normal to high-strength concrete. Based on the experimental results, an analytical expression of normal and high-strength steel fiber concrete confined by transversal reinforcement will be developed.

2. Program of experiment

2.1 Concrete materials

SNI 7656-2012 is a reference for the concrete mix design. Concrete materials are designed and divided into three water-cement (*w*/*c*) ratio categories: 0.53, 0.38, and 0.28 (Table 1). The three types of *w*/*c* are designed to produce normal-strength concrete, medium-strength concrete, and high-strength concrete.

The concrete mix design above incorporates an additive, specifically Sika@ViscoCrete@-3115N, to enhance workability. Each concrete mix at various *w*/*c* ratios consists of several specimens with varying percentages of steel fiber (0%, 1%, 2%) by volume.

2.2 Specimens

Reinforced concrete cylinder specimens using 4ϕ7.6 longitudinal reinforcement and circular hoop as confining reinforcement (5.5 mm diameter). The results of the tensile test of the reinforcing bars are presented in Table 2. The specimens have a diameter of 100 mm, and a height of 200 mm without using a concrete cover. The steel fiber used was simple steel fiber cut from steel wire in such a way that results *l*/*d* ratio between 50 and 60 (Fig. 1(a)). Confined concrete specimens review the design parameters of the steel fiber fraction volume (V_f), which consists of V_f = 0% (without fiber or so-called normal concrete), V_f = 1% and V_f = 2%, concrete compressive strength (f_c'), and hoops spacing of 50 mm and 100 mm (Figs. 1(b) and 1(c)). Mixing fiber with concrete is carried out by gradually sowing the fiber when casting the concrete.

2.3 Instrumentation and data acquisition

Specimen deformation in the axial direction was measured by installing four LVDTs in the test area. Strain gage type FLA-6-11 is installed on the longitudinal reinforcement and hoop. The cables from the LVDT and the strain gauge are then connected to the Data Logger. Uniaxial loading uses a compression testing machine with an effective capacity of 1800 kN and a Deformation Control testing system, and it is carried out in stages. Cylinder testing standards follow ASTM C 39–94. The confined

Table 1 Concrete mix design

Materials	*w*/*c* = 0.53	*w*/*c* = 0.38	*w*/*c* = 0.28
Cement (kg/m^3)	350	420	485
Fly Ash (kg/m^3)	-	72	83
Water (lt/m^3)	186	160	136
Sand (kg/m^3)	723	647	622
Coarse aggregate (kg/m^3)	887	1045	1086
Viscocrete (kg/m^3)	1.75	9.84	14.19

Table 2 Reinforcing steel tensile test result

Reinforcement	Diameter (mm)	Yield stress (MPa)
Hoop	5.5 mm	384
Longitudinal reinf.	7.6 mm	432

(a) Steel fiber (b) Longitudinal reinf. and hoop (s = 50 mm) (c) Longitudinal reinf. and hoop (*s* = 100 mm)

Fig. 1 Steel fiber and reinforcement

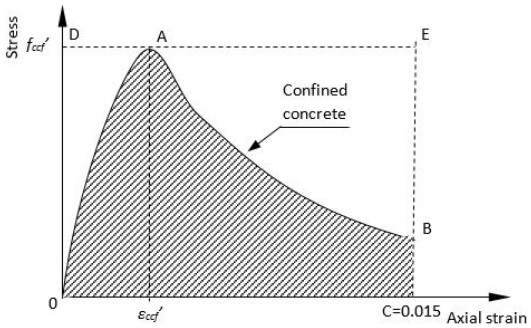

Fig. 2 Definition of toughness index

concrete stress (f_{cc}) is the total load received by the specimen minus the load received by the longitudinal reinforcement which is calculated based on the strain data. The strength enhancement of confined concrete (*K*) is defined as the ratio between the confined concrete stress at peak response and the unconfined concrete stress. The value of *K* is a primary focus of this research because it plays a significant role in determining the minimum volumetric ratio of confining reinforcement required for its application in column structures. The unconfined concrete stress is defined as 85% of the cylindrical concrete stress with a diameter of 150 mm and height of 300 mm. In this study, the energy method is used to calculate the ductility of confined concrete, namely the Toughness Index (*TI*) (Aoude *et al*. 2014, Antonius 2015). The *TI* calculation is defined as the ratio of the OABC area (shaded) to the ODEC area (Fig. 2).

Table 3 Experimental results

Specimen	V_f (%)	f_c' (MPa)	f_{cf}' (MPa)	ε_{cf}'	Hoop/confined		f_{ccf}' (MPa)	$K = \frac{f_{ccf}'}{0.85 f_{cf}'}$	*TI*
					ϕ-*s* (mm)	ε_h (at peak response)			
SFC1	0		34.9	0.0022		yield	30.71	1.04	0.32
SFC2	1	34.9	40.9	0.004	5.5-100	yield	38.45	1.11	0.32
SFC3	2		41.2	0.0051		yield	40.38	1.15	0.56
SFC4	0	50.6	50.6	0.003	5.5-100	0.0019	41.83	0.98	0.40
SFC5	0		70.5	0.0035		0.0012	57.11	0.95	0.30
SFC6	1	70.5	71.1	0.0053	5.5-100	0.0012	63.99	1.06	0.45
SFC7	2		80.6	0.0067		yield	73.35	1.07	0.56
SFC8	0		34.9	0.0022		yield	38.14	1.29	0.41
SFC9	1	34.9	40.9	0.004	5.5-50	yield	44.83	1.29	0.54
SFC10	2		41.2	0.0051		yield	45.64	1.30	0.80
SFC11	0	50.6	50.6	0.003	5.5-50	yield	54.56	1.27	0.49
SFC12	1		57	0.0034		yield	62.47	1.29	0.65
SFC13	0		70.5	0.0035		yield	73.52	1.23	0.55
SFC14	1	70.5	71.1	0.0053	5.5-50	0.0019	75.89	1.26	0.83
SFC15	2		80.6	0.0067		0.0015	86.77	1.27	0.88

Specimen f_c'= 3 4.5 MPa, hoop spaced = 50 mm

Specimen f_c' = 50.6 MPa, hoop spaced = 50 mm

Specimen f_c' = 70.5 MPa, hoop spaced = 50 mm

Specimen f_c' = 34.5 MPa, hoop spaced = 100 mm

Specimen f_c' = 50.6 MPa, hoop spaced = 100 mm

Specimen f_c' = 70.5 MPa, hoop spaced = 100 mm

Fig. 3 Specimen collapse mode

3. Experimental results and discussion

The experimental results are presented in Table 3. In the table, the f_c' dan f_{cf}' values represent the compressive strength of cylindrical concrete with a diameter of 150 and a height of 300 mm without reinforcement. Each is concrete without fiber (V_f = 0%) and concrete with fiber ($V_f \neq 0$). The table also indicates that from the results of the compressive strength test, three categories of concrete compressive strength were obtained, namely normal-strength (f_c' = 34.9 MPa), medium-strength (f_c' = 50.6 MPa) and high-strength (f_c' = 70.5 MPa). Based on Table 3, it can be seen that not all hoops have yielded at the peak response. Specimens without steel fiber and steel fiber concrete confined by hoops with the same spacing as the specimen diameter of 100 mm, namely SFC4, SFC5, and SFC6. Those are specimens where the attached hoops have not yielded peak response.

As seen in Table 3, all hoop reinforcements have yielded in specimens made of normal-strength concrete (SFC1, SFC2, SFC3, SFC8, SFC9, SFC10). In the case of medium-strength concrete specimen SF4, this value approaches its yield strain at the peak strain response of hoop reinforcement (0.0019).

In addition to the hoops on the three specimens above, the hoops are also attached to specimens containing steel fibers that have not yielded during peak response (i.e., SFC6, SFC14, SFC15). The three specimens have a value of f_c' = 70.5 MPa, which is included in the category of high-strength concrete. The behavior of the transversal reinforcement as a confinement at peak response of confined steel fiber concrete indicates that yield is not always reached. This phenomenon has been described equally by Razvi and Saatcioglu (1999). However, the study was limited to high-strength concrete without fiber content.

Another result shown in Table 3 is the ductility of confined concrete expressed in the amount of *TI*. Steel fiber plays a significant role in determining the value of *TI*. The higher the volume of the fiber fraction, the higher the value of *TI*. It is unaffected by whether or not the hoop has yielded at the time of peak response. These results are based on comparing specimens with the same concrete compressive strength and hoops with the same spacing.

Fig. 3 shows the specimen's failure pattern due to uniaxial compressive loads. It can be visually stated that specimens mounted with hoops with wider spacing (s = 100 mm) experience more brittle collapse compared to specimens mounted with tighter spacing (s = 50 mm). Another phenomenon is that specimens containing steel fibers tend to collapse relatively more ductile than specimens without steel fibers (V_f = 0%).

3.1 Concrete cylinders without steel reinforcement

Specimens containing a higher volume fraction of steel fiber improve failure patterns, especially from macro-cracks to micro-cracks. The behavior is in line with the research results conducted by Abubakar and Akcaoglu (2021). As shown in Table 3, strength results for cylindrical concrete without reinforcement are present. Fig. 4 shows a diagram of the relationship between the normalized compressive strength of fibrous concrete cylinders (f_{cf}') to normal concrete compressive strength (f_c') and the volume of steel fiber fractions. It can be seen in Fig. 4 that steel fiber influences the increase compressive strength of the concrete. The concrete's compressive strength increases when the steel fiber fraction volume rises. This phenomenon occurs in normal, medium, and high-strength concrete cylinders. In addition to compressive strength, another role in the presence of steel fibers represents the increase in the peak strain of the concrete, as shown in Fig. 5. This indicates that the deformability properties of steel fiber specimens are getting better as the volume of the fiber fraction increases.

This behavior indicates a better and higher ductility due to the addition of the volume of the steel fiber fraction.

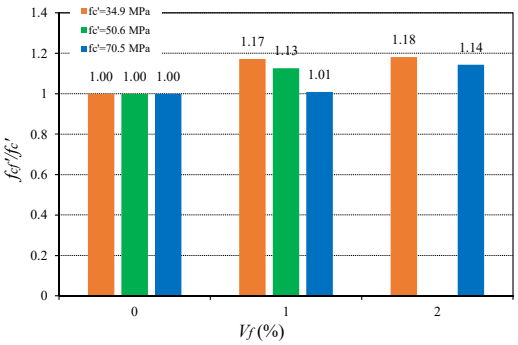

Fig. 4 Influence of fraction volume to the compressive strength

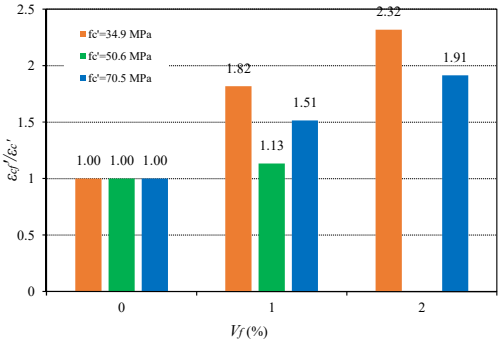

Fig. 5 Influence of fraction volume to the strain

3.2 Confined concrete

3.2.1 Strength enhancement of confined concrete (*K*)

Fig. 6 shows a comparison of increasing K values with increasing volume of the steel fiber fraction in confined concrete specimens. The comparison is performed between specimens with concrete compressive strength and the same spacing. In addition, in normal compressive strength concrete (f_c' = 34.9 MPa) or the comparison between the orange and gray diagrams. The K value increases significantly when considering the effect of the hoop spacing installed. The effect of this spacing is the same as that of high-strength concrete (f_c' = 70.5 MPa) or the comparison between the blue and green bar diagrams in Fig. 6.

3.2.2 Stress-strain behavior

The stress-strain behavior of confined concrete is evaluated by reviewing the volume parameters of the steel fiber fraction and the effect of concrete compressive strength and hoop spacing. As shown in Fig. 7, the value of K increases and the post-peak curve becomes more sloping as the volume of the fiber fraction increases. Variations in

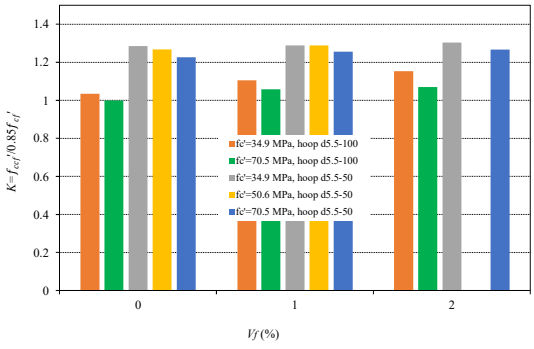

Fig. 6 Comparison of K value results

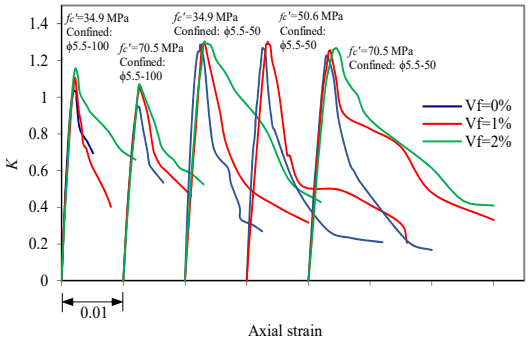

Fig. 7 Influence of fraction volume on the confined concrete behavior

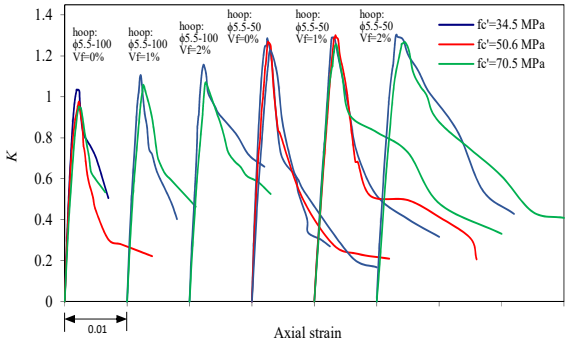

Fig. 8 Influence of concrete strength on confined concrete behavior

the compressive strength of concrete generally have no significant effect on the post-peak response of the confined concrete (Fig. 8). Similar to the behavior of confined concrete without steel fibers, the behavior of specimens with closer hoop spacing has a higher K value. In addition, the specimens are also more ductile compared to specimens with wider spacing. Typically, this behavior applies when comparing specimens with the same compressive strength and fiber volume fraction (Fig. 9).

Table 4 Confinement models

Model	Peak stress and peak strain	Stress-strain curves	Parameter equations
Ganesan & Murthy	$K = 1 + \frac{\rho_s f_{yh}}{f_c'}$ $e_p = 0.002K(1 + V_f A_p)$	Ascending branch: $f = Kf_{cf}' \frac{A_1\left(e/e_p\right) + B_1\left(e/e_p\right)^2}{1 + C_1\left(e/e_p\right) + D_1\left(e/e_p\right)^2}$ Descending branch: $f = Kf_{cf}' \frac{A_2\left(e/e_p\right) + B_2\left(e/e_p\right)^2}{1 + C_2\left(e/e_p\right) + D_2\left(e/e_p\right)^2}$	$A_1 = 3.566 - 0.84473(\rho_s)$ $B_1 = 0.963 - 0.22808(\rho_s)$ $C_1 = 0.597 - 0.09675(\rho_s)$ $D_1 = 2.214 - 0.44384(\rho_s)$ $A_2 = -5.885 + 1.12404(\rho_s)$ $B_2 = 5.318 - 1.52414(\rho_s)$ $C_2 = -8.529 + 1.82759(\rho_s)$ $D_2 = 4.916 - 0.70236(\rho_s)$
Campione	$\frac{f_{cc}'}{f_c'} = 1 + 2.1\left(k_e \frac{f_l}{f_c'}\right)^{0.7}$ $\frac{\varepsilon_{cc}}{\varepsilon_o} = 1 + 5k_1\left(k_e \frac{f_l}{f_c'}\right)^{0.7}$	$\frac{\sigma}{f_c'} = \frac{\beta(\varepsilon/\varepsilon_0)}{\beta - 1 + (\varepsilon/\varepsilon_0)^{\beta}} \dots\dots\dots\dots\dots (a)$ $\frac{\sigma}{f_c'} = \eta_d exp\left[-k_d\left(\frac{\varepsilon}{\varepsilon_o} - x_d\right)^{\gamma}\right] \dots\dots (b)$	$\beta = A + B(RI)^C$ where $A = 0.5811$ $B = 1.93$, $C = -0.740$ $\beta = \frac{E_c}{E_c - \left(f_c'/\varepsilon_o\right)}$ η_d, k_d, x_d, γ are constant influenced by volumetric ratio of confinement and fraction volume of fiber
Naeimi & Moustafa	$f_{cc}' = f_{co'\,vf=0} + 6.26v_f + 6.57\rho_s$ (MPa) $\varepsilon_{cc}' = \varepsilon_{co'\,vf=0} + 7.82.10^{-5}6v_f + 3.49.10^{-4}\rho_s$	Zone 1: $f_c = f_{cc}' \frac{\beta_1\left(\frac{\varepsilon_c}{\varepsilon_{cc'}}\right)}{\beta_1 - 1 + \left(\frac{\varepsilon_c}{\varepsilon_{cc}}\right)^{\beta_1}}$ for $\frac{\varepsilon_c}{\varepsilon_{cc}'} \le 1.0$ Zone 2: $f_c = f_{cc}' \frac{\beta_2\left(\frac{\varepsilon_c}{\varepsilon_{cc'}}\right)}{\beta_2 - 1 + \left(\frac{\varepsilon_c}{\varepsilon_{cc}}\right)^{\beta_3}}$ Zone 3: For $1.0 \le \frac{\varepsilon_c}{\varepsilon_{cc}'} \le \chi_d$ Zone 3: $f_c = \eta_d f_{cc}' \left[e^{-k_1\left(\frac{\varepsilon_c - \varepsilon_d}{\varepsilon_{cc}'}\right)}\right]^{k_2}$ For $x_d \le \frac{\varepsilon_c}{\varepsilon_{cc}'}$	$\beta_1 = \frac{1}{1 - \frac{f_{cc'}}{\varepsilon_{cc'}E_c}}$ $\varepsilon_{co'\,vf=0} = 2.54.10^{-5}.f_{co'\,vf=0}$ $\eta_d = 0.289 + 0.004v_f + 0.052\rho_s$ $\chi_d = \frac{\varepsilon_{cc,d}}{\varepsilon_{cc}'}$ $\varepsilon_{cc,d} = \frac{\eta_d}{f_{cc}'}$ $\beta_2 = 3.096 - 0.0941v_f - 0.2073\rho_s$ $\beta_3 = 3.793 - 0.2314v_f - 0.010\rho_s$ $k_1 = 0.2392 + 0.0112v_f - 0.0207\rho_s$ $k_2 = 0.8975 + 0.0613v_f - 0.0129\rho_s$ $E_c = 3400\sqrt{f_{co'\,vf=0\%}} + 1310v_f\ MPa$

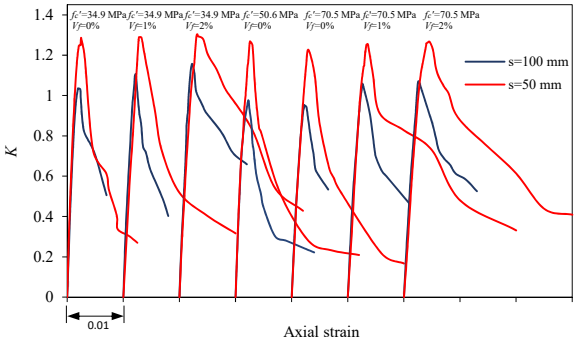

Fig. 9 Influence of spacing of hoop on the confined concrete behavior

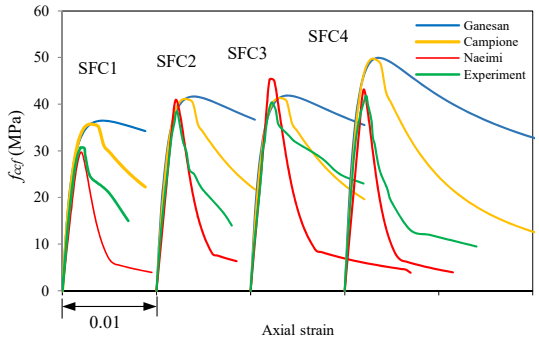

Fig. 10 Confinement models vs experiment (SFC1, SFC2, SFC3, SFC4)

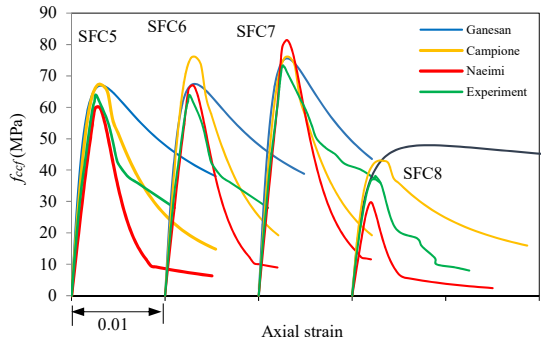

Fig. 11 Confinement models vs experiment (SFC5, SFC6, SFC7, SFC8)

3.2.3 Comparison of confinement models with experimental result

Further, the stress-strain behavior of confined concrete from the experimental results above will be compared with the present models of confinement of fibrous concrete. The selected models are shown in Table 4.

The confinement model proposed by Ganesan and Murthy (1990) was derived from testing eight small-scale column specimens containing a 1.5% fiber volume fraction. The Ganesan model divides the stress-strain curve into two parts: the ascending and descending branches. The coefficients A, B, C, and D represent a function of the volumetric ratio of the confining reinforcement (ρ_s). The K equation represents a function of the compressive strength of the concrete, the volumetric ratio, and the yield stress of the confining reinforcement used. Additionally, the proposed confinement model by Ganesan assumes that the confining reinforcement has yielded at the peak response. Ganesan proposed the peak strain equation for confined concrete influenced by the K value, the fiber's volume fraction, and the fiber's aspect ratio.

The confinement model proposed by Campione (2002) was derived from a number of experimental results of concrete containing a zero to 3% volume fiber fraction. Fundamentally, the Campione model is a modification of the previous confinement model by Hsu and Hsu (1994).

The confinement model for fiber-reinforced concrete proposed by Campione includes equations for normal-strength and high-strength concrete. For normal-strength concrete, as shown in Table 4, equation (a) is used, where a single equation represents the pre- and post-peak curves. The shape of this curve is influenced by the value of β, which is affected by the magnitude of the Reinforcing Index (RI). According to Campione, the values of A, B, and C for crimped steel fibers are specified in Table 4. He proposes a stress-strain curve divided into two parts for high-strength concrete, as shown in Table 4. The first part is the ascending branch, represented by equation (a), and the second is the descending branch, represented by equation (b). The experimental results also derive the stress-strain equations for confined concrete peaks. They are influenced by the k_e, f_l, and f_c' parameters, where, according to Campione, the value of k_e differs for spiral and hoop confining reinforcement. Based on the equations f_{cc}'/f_{co}' dan $\varepsilon_{cc}/\varepsilon_{co}$, it is evident that the confining reinforcement is assumed to have yielded at the peak response.

The model by Naeimi and Moustafa (2021) was derived after testing ultra-high strength steel fiber concrete. The volume fraction of fiber used is from zero to 4%. Naemi derives the peak stress and peak strain equations for confined concrete from the experimental results, where both equations are affected by the fiber's volume fraction and the confining reinforcement's volumetric ratio. In contrast to the two confinement models of fibrous concrete described above, the model proposed by Naeimi divides the stress-strain curve into three regions. The first area is the pre-peak curve. The second area is after the peak response to the value $\varepsilon_{cc,d}$, and the third is after the strain value $\varepsilon_{cc,d}$. The equations f_{cc}' and ε_{cc}' show that the fiber volume fraction and the volumetric ratio of confining reinforcement directly influence these values. The confinement model by Naeimi does not indicate any influence of the yield stress and lateral stress of the confining reinforcement on the magnitudes of f_{cc}' dan ε_{cc}'.

Figs. 10 to 13 shows the results of comparing the stress-strain behavior of confined steel fiber concrete. The pre-peak curves between all models with experimental results coincide relatively with each other. In the post-peak curves and fccf' value, the Ganesan model significantly differs from the experimental results. Meanwhile, the post-peak behavior between Campione's model and the corresponding experimental results differs, except for specimens SFC 12 and SFC 13.

The Naeimi model has the shape of a post-peak curve and f_{ccf}', which is not too far from the experimental results

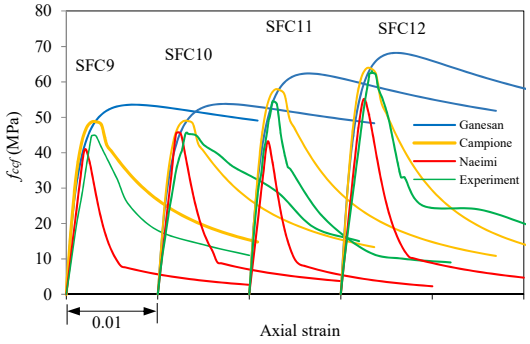

Fig. 12 Confinement models vs experiment (SFC9, SFC10, SFC11, SFC12)

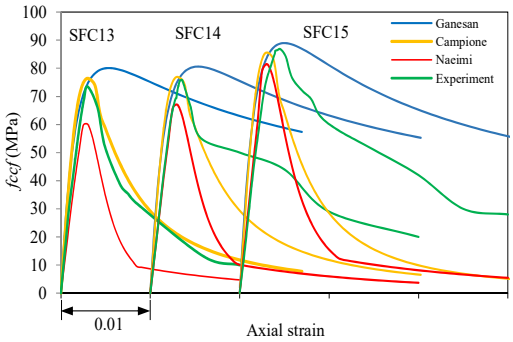

Fig. 13 Confinement models vs experiment (SFC13, SFC14, SFC15)

when comparisons are made on specimens installed with hoops with a spacing of 100 mm (SFC1, SFC2, SFC3, SFC4, SFC5, SFC6, SFC7). However, the post-peak curve of the Naeimi model begins deviating significantly from the experimental results curve if the applied stress has dropped by about 50%. In a comparison of the Naeimi model with other experimental results, the post-peak stress-strain curves (including f_{ccf}') and the experimental results differ greatly when the specimens are hooped with a spacing of 50 mm (SFC8, SFC9, SFC10, SFC11, SFC12, SFC13, SFC14, SFC15).

The accuracy of the reviewed confinement models in predicting the experimental values of *K* and *TI* was assessed using a statistical approach. Table 5 shows that the model proposed by Campione is the closest in predicting the values of *K* and *TI*, with the resulting COV values being 11.7% and 32.7%, respectively.

4. Analytical expression of confined normal and high-strength steel fiber concrete

An analytical expression of confined steel fiber concrete is needed to model the prior experimental results in general. Until now, several stress-strain models of fibrous concrete have been proposed, such as those proposed by Ezeldin and Balaguru (1992), Nataraja *et al*. (1999), Ou *et al*. (2012), Liao *et al*. (2015). In this paper, the analytic expression developed adopts and modifies some equations from present models. The confined concrete stress-strain curve is modeled in one step only, and the Ezeldin proposed equation is used as follows

$$\frac{f_{cf}{}'}{f_{ccf}{}'} = \frac{\beta\left(\frac{\varepsilon_{cf}}{\varepsilon_{ccf'}}\right)}{\beta - 1 + \left(\frac{\varepsilon_{cf}}{\varepsilon_{ccf'}}\right)^{\beta}} \quad (1)$$

Table 5 Statistical approach of K and TI for confinement models vs experiment

Specimen	*K*				*TI*			
	Experiment	Ganesan	Campione	Naeimi	Experiment	Ganesan	Campione	Naeimi
SFC1	1.04	1.23	1.2	1	0.32	0.86	0.65	0.28
SFC2	1.11	1.2	1.18	1.18	0.32	0.89	0.66	0.29
SFC3	1.15	1.2	1.18	1.35	0.56	0.89	0.66	0.31
SFC4	0.98	1.16	1.15	1	0.4	0.86	0.62	0.26
SFC5	0.95	1.12	1.12	1	0.3	0.78	0.54	0.36
SFC6	1.06	1.11	1.12	1.01	0.45	0.75	0.54	0.38
SFC7	1.07	0.98	0.98	1.06	0.56	0.71	0.49	0.4
SFC8	1.29	1.61	1.4	1	0.41	0.91	0.68	0.28
SFC9	1.29	1.54	1.4	1.18	0.54	0.91	0.64	0.29
SFC10	1.3	1.54	1.4	1.17	0.8	0.91	0.64	0.32
SFC11	1.27	1.45	1.34	1	0.49	0.9	0.6	0.27
SFC12	1.29	1.41	1.31	1.14	0.65	0.89	0.6	0.34
SFC13	1.23	1.34	1.27	1	0.55	0.88	0.53	0.36
SFC14	1.26	1.33	1.27	1.11	0.83	0.88	0.53	0.38
SFC15	1.27	1.3	1.25	1.18	0.88	0.86	0.49	0.41
Mean		1.30	1.238	1.092	Mean	0.859	0.591	0.329
SD		0.183	0.144	0.15	SD	0.382	0.193	0.797
COV (%)		14.1	11.7	13.78	COV (%)	44.5	32.7	242.4

if $V_f = 0\%$, the β value of Eq. (1) uses the equation proposed by Junior *et al*. (2010) namely

$$\beta = \left(0.0536 - 0.5754 V_f\right) f_c{}' \tag{2}$$

And if $V_f \neq 0$, the value of β adopts the equation proposed by Nataraja *et al*. (1999), namely

$$\beta = 0.5811 + 1.93\ (RI)^{-0.7406} \tag{3}$$

where

$$RI = 3.2\, V_f \left(l/d\right) \tag{4}$$

The experimental results above reveal an increase in the compressive strength of concrete due to the rise in the volume of the steel fiber fraction. Therefore, the compressive strength equation for steel fiber concrete is used, which is a function of the normal concrete compressive strength plus the fiber contribution stated in the reinforced index (*RI*), namely the proposal of Nataraja *et al*. (1999) below

$$f_{cf}{}' = f_{co}{}' + 2.1604\ (RI) \tag{5}$$

where

$$f_{co\prime} = 0.85\, f_c{}' \tag{6}$$

And the top strain of confined steel-fiber concrete

$$\varepsilon_{ccf}{}' = \varepsilon_{cf}{}' + 0.0006\ (RI) \tag{7}$$

The peak strain of unconfined fiber concrete is a modification of Antonius *et al*. (2017) proposed equation, thus

$$\varepsilon_{cf}{}' = 0.0004\ \left(f_{cf}{}'\right)^{0.45} \tag{8}$$

In addition to what has been mentioned in Table 4 above, up to the present time there have been many proposed equations for increasing confined steel fiber concrete (*K*), including the proposal by Pantazopulou and Zanganeh (2001) resulting from triaxial testing of fibrous concrete. Cholida *et al*. (2022) used this equation to predict *K* values. On the other hand, Paultre *et al*. (2010) derived the K equation using the experimental data he did. In this study, the equation for the value of *K* proposed by Pantazopoulou & Zanganeh is adopted to predict the peak stress of confined steel fiber reinforced concrete. The resulting equation is

$$f_{ccf}{}' = 0.85\, f_{cf}{}' \left(1 + 3.5\, \frac{f_{le}}{0.85 f_{cf}{}'}\right) \tag{9}$$

The following equation calculates the lateral stress due to the confining reinforcement

$$f_l = \frac{2\ A_{sh}\ f_y}{s\ d_c} \tag{10}$$

Based on Eq. (10) above, the hoop reinforcement is assumed to have yielded at its peak response. The lateral stress value of Eq. (10) above is multiplied again by the effectiveness coefficient of the confinement (k_e), where for circular cross-section, the effectivity of confinement between hoops and spirals is the same (Antonius *et al*. 2017). The equation proposed by Mander *et al*. (1988) adopted, namely

$$k_e = \frac{\left(1 - \frac{A\prime}{2d}\right)}{1 - \rho_{cc}} \tag{11}$$

So, the effective lateral stress is

$$f_{le} = k_e \,.\, f_l \tag{12}$$

The analytical expressions developed above are compared with all confined concrete specimens shown in

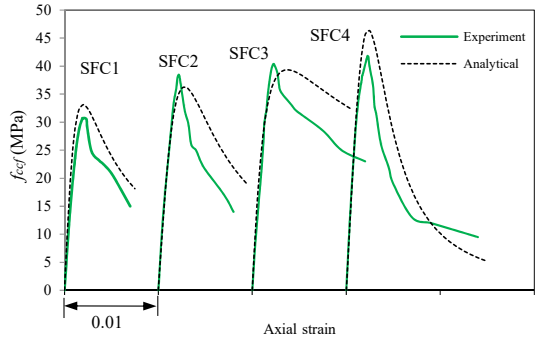

Fig. 14 Analytical vs experimental results (SFC1, SFC2, SFC3, SFC4)

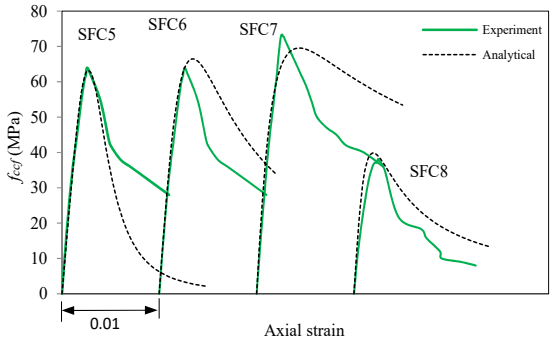

Fig. 15 Analytical vs experimental results (SFC5, SFC6, SFC7, SFC8)

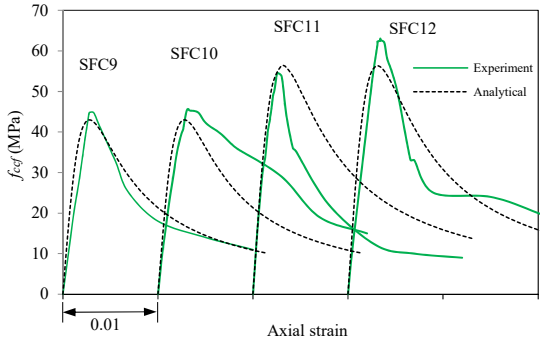

Fig. 16 Analytical vs experimental results (SFC9, SFC10, SFC11, SFC12)

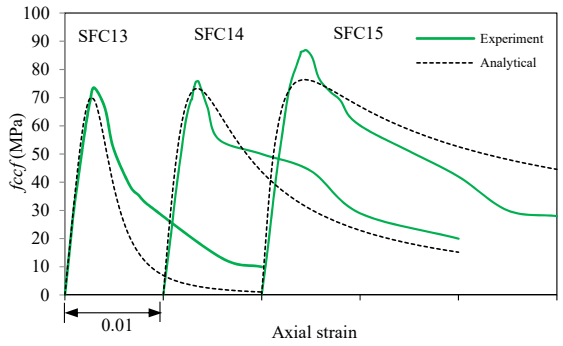

Fig. 17 Analytical vs experimental results (SFC13, SFC14, SFC15)

Table 6 Statistical approach of *K* and *TI* for analytical expression vs experiment

Specimen	*K*		*TI*	
	Experiment	Analytical	Experiment	Analytical
SFC1	1.04	1.12	0.32	0.57
SFC2	1.11	1.10	0.32	0.62
SFC3	1.15	1.10	0.56	0.83
SFC4	0.98	1.08	0.4	0.42
SFC5	0.95	1.05	0.3	0.33
SFC6	1.06	1.05	0.45	0.67
SFC7	1.07	1.05	0.56	0.85
SFC8	1.29	1.34	0.41	0.58
SFC9	1.29	1.31	0.54	0.62
SFC10	1.3	1.28	0.8	0.83
SFC11	1.27	1.22	0.49	0.64
SFC12	1.29	1.22	0.65	0.65
SFC13	1.23	1.17	0.55	0.33
SFC14	1.26	1.17	0.83	0.67
SFC15	1.27	1.15	0.88	0.85
Mean		1.160		0.631
SD		0.126		0.196
COV (%)		10.8		31.1

Figs. 14 to 17. The comparison results show that the analytical expression can predict relatively the stress-strain behavior of confined normal-strength to high-strength concrete containing steel fiber, except for specimen SFC7.

Furthermore, the *COV* values generated for predicting *K* and *TI* are 10.8% and 31.1% (Table 6), respectively. These *COV* values are lowest compared to the *COV* values based on the existing models above, indicating that the analytical expression is closest to the experimental results.

5. Conclusions

The stress-strain behavior of confined normal and high-strength steel fiber concrete has been presented in this paper. The conclusions can be written as follows:

- In most cases, adding steel fiber can increase the compressive strength of concrete without reinforcement. Likewise, in confined steel fiber concrete, the volume fraction of steel fiber plays an important role in improving the *K* value and the ductility of confined concrete.
- The optimum *K* value will be used for concrete with normal compressive strength (f_c' = 34.9 MPa). Conversely, the *K* value decreases for specimens with higher concrete compressive strength.
- Hoop reinforcement is important in determining confined steel fiber concrete's *K* value and ductility. The *K* value and the ductility increase when the hoops are more tightly spaced.
- The existing fiber confinement models evaluated in this study were able to predict the experimental pre-peak behavior well. However, in most cases, these models experience significant differences with experimental results in predicting confined concrete's peak stress and post-peak behavior.
- The developed analytical expression produces a stress-strain curve for confined concrete that closely matches the stress-strain behavior of most specimens.
- This research can however be developed more considerably by reviewing broader design parameters such as square cross sections, effects of reinforcement configurations, and structures subjected to cyclic loads. Therefore, the analytical expression for confined steel fiber reinforced concrete mentioned above still needs to be further tested and refined through future research.

Acknowledgments

This paper results from research funded by Universitas Islam Sultan Agung-Indonesia (Contract No.322/B.1/SA-LPPM/IX/2022) in collaboration with Universitas Semarang-Indonesia and fib-Indonesia. The support received for this research is gratefully acknowledged.

References

Abubakar, A.U. and Akcaoglu, T. (2021), "Influence of pre-compression on crack propagation in steel fiber reinforced concrete", *Adv. Concrete Constr., Int. J.*, **11**(3), 261-270. https://doi.org/10.12989/acc.2021.11.3.261

ACI Committee 318 (2019), Building Code Requirements for Structural Concrete (ACI-318-19) and Commentary (318R-19), American Concrete Institute, Farmington Hills, MI, USA.

Al-Tikrite, A. and Hadi, M.N.S. (2018), "Influence of steel fibres on the behaviour of RPC circular columns under different loading conditions", *Structures*, **14**, 111-123. https://doi.org/10.1016/j.istruc.2018.03.002

Amariansah, W. and Karlinasari, R. (2019), "The influence of steel fiber on the stress-strain behavior of confined concrete", *J. Adv. Civil Environ. Eng.*, **2**(1), 46-52. https://doi.org/10.30659/jacee.2.1.46-52

Antonius (2015), "Strength and energy absorption of high-strength steel fiber concrete confined by circular hoops", *Int. J. Technol.*,

6(2), 217-226. https://doi.org/10.14716/ijtech.v6i2.860
Antonius, Imran, I. and Setiyawan, P. (2017), "On the confined high-strength concrete and need of future research", *Procedia Eng*., **171**, 121-130. https://doi.org/10.1016/j.proeng.2017.01.318
Antonius, Purwanto and Harprastanti, P. (2019), "Experimental study of the flexural strength and ductility of post burned steel fiber RC beams", *Int. J. Technol*., **10**(2), 428-437. https://doi.org/10.14716/ijtech.v10i2.2097
Antonius, Karlinasari, R., Purwanto and Widhianto, A. (2020), "Shear strength and deformation of steel fiber reinforced concrete beams after fire", *Adv. Concrete Constr*., *Int. J*., **10**(2), 105-111. https://doi.org/ 10.12989/acc.2020.10.2.105
Aoude, H., Hosinieh, M.M., Cook, W.D. and Mitchell, D. (2014), "Behaviour of rectangular columns constructed with SCC and steel fibers", *J. Struct. Eng*., **141**(8), 04014191. https://doi.org/10.1061/(ASCE)ST.1943-541X.0001165
ASTM C 39–94 (1996), Test Method for Compressive Strength of Cylindrical Concrete Specimens. Annual Books of ASTM Standards, USA.
Campione, G. (2002), "The effects of fibers on the confinement models for concrete columns", *Can. J. Civil Eng*., **29**, 742-750. https://doi.org/10.1139/l02-066
Cholida, N.F.F., Antonius and Enggartiasto, L. (2022), "A comparative study of the confinement models of high-strength steel fiber concrete by statistical approach", *J. Civil Eng. Forum*, **8**(3), 309-320. https://doi.org/10.22146/jcef.4029
Ezeldin, A.S. and Balaguru. P.N. (1992), "Normal- and high-strength fiber-reinforced concrete under compression", *J. Mater. Civil Eng*., **4**, 415. https://doi.org/10.1061/(ASCE)0899-1561(1992)4:4(415)
García-Taengua, E., Martí-Vargas, J.R. and Serna, P. (2014), "Splitting of concrete cover in steel fiber reinforced concrete: semi-empirical modeling and minimum confinement requirements", *Constr. Build. Mater*., **66**, 743-751. https://doi.org/10.1016/j.conbuildmat.2014.06.020
Gomes, L.D. dos Santos, Oliveira, D.R.C., Neto, B.N. de Moraes, Medeiros, A.B., Macedo, A.N. and Silva, F.A.C. (2018), "Experimental analysis of the efficiency of steel fibers on shear strength of beams", *Latin Am. J. Solids Struct*., **15**, 1-16. https://doi.org/10.1590/1679-78254710
Ganesan, N. and Murthy, J.V.R. (1990), "Strength and behavior of confined steel fiber reinforced concrete columns", *ACI Mater. J*., **87**(3), 221-227. https://www.concrete.org/publications/acimaterialsjournal.aspx
Han, A.L., Antonius and Okiyarta, A.W. (2015), "Experimental study of steel fiber reinforced concrete beams with confinement", *Procedia Eng*., **125**, 1030-1035. https://doi.org/10.1016/j.proeng.2015.11.158
Hsu, L.S. and Hsu, C.T. (1994), "Stress-strain behavior of steel-fiber high-strength concrete under compression", *ACI Struct. J*., **91**(4), 448-457. https://doi.org/10.14359/4152
Indonesian National Standard, SNI 2847-2019, Requirements of Structural Concrete for Buildings (in Indonesian).
Indonesian National Standard, SNI 7656:2012, Procedures of Mixed Selection for Normal Concrete, Heavy Concrete and Mass Concrete (in Indonesian).
Jang, S.J. and Yun, H.D. (2018), "Combined effects of steel fiber and coarse aggregate size on the compressive and flexural toughness of high-strength concrete", *Compos. Struct*., **185**, 203-211. https://doi.org/10.1016/j.compstruct.2017.11.009
Junior, L.A.O., do Santos Borges, V.E., Danin, A.R. and Machado, D.V.R. (2010), "Stress-strain curves for steel fiber-reinforced concrete in compression", *Revista Materia*, **15**(2), 260-266. https://doi.org/10.1590/S1517-70762010000200025
Liao, W.C., Perceka, W. and Liu, E.J. (2015), "Compressive stress-strain relationship of high strength steel fiber reinforced concrete", *J. Adv. Concrete Technol*., **13**, 379-392. https://doi.org/10.3151/jact.13.379
Lu, X., Zhang, Y. and Zhang, H. (2018), "Experimental study on seismic performance of steel fiber reinforced high strength concrete composite shear walls with different steel fiber volume fractions", *Eng. Struct*., **171**, 247. https://doi.org/10.1016/j.engstruct.2018.05.068
Mander, J.B., Priestley, M.J.N. and Park, R. (1988), "Theoretical stress-strain model for confined concrete", *J. Struct. Eng*., **114**(8), 1804-1826. https://doi.org/10.1061/(ASCE)0733-9445(1988)114:8(1804)
Mansouri, I., Shahheidari, F.S., Hashemi, S.M.A. and Farzampour, A. (2020), "Investigation of steel fiber effects on concrete abrasion resistance", *Adv. Concrete Constr*., *Int. J*., **9**(4), 367-374. https://doi.org/10.12989/acc.2020.9.4.367
Naeimi, N. and Moustafa, M.A. (2021), "Analytical stress–strain model for steel spirals-confined UHPC", *Compos. Part C*: *Open Access*, **5**, 100130. https://doi.org/10.1016/j.jcomc.2021.100130
Nataraja, M.C., Dhang, N. and Gupta, A.P. (1999), "Stress-strain curves for steel-fiber reinforced concrete under compression", *Cement Concrete Compos*., **21**, 383-390. https://doi.org/10.1016/S0958-9465(99)00021-9
Ou, Y.C., Tsai, M.S., Liu, K.Y. and Chang, K.C. (2012), "Compressive behavior of steel fiber reinforced concrete with a high reinforcing index", *J. Mater. Civil Eng*., **24**, 207-215. https://doi.org/10.1061/(ASCE)MT.1943-5533.0000372
Pantazopoulou, S.J. and Zanganeh, M. (2001), "Triaxial tests of fiber-reinforced concrete", *J. Mater. Civil Eng*., **13**(5), 340-348. https://doi.org/10.1061/(ASCE)0899-1561(2001)13:5(340)
Paultre, P., Eid, R., Langlois, Y. and Lévesque, Y. (2010), "Behavior of steel fiber-reinforced high-strength concrete columns under uniaxial compression", *J. Struct. Eng*., **136**(10), 1225-1235. https://doi.org/10.1061/(ASCE)ST.1943-541X.0000211
Purwanto, Antonius and Setiyawan, P. (2021), "Stress-strain behavior of normal and high-strength steel fiber concrete post burning", *Int. J. GEOMATE*, **21**(85), 61-70. https://doi.org/10.21660/2021.85.j2211
Rabi, M., Cashell, K.A., Shamass, R. and Desnerck, P. (2020), "Bond behaviour of austenitic stainless steel reinforced concrete", *Eng. Struct*., **221** p. 111027. https://doi.org/10.1016/j.engstruct. 111027
Razvi, S. and Saatcioglu, M. (1999), "Confinement model for high-strength concrete", *J. Struct. Eng*., **125**(3), 281-289. https://doi.org/10.1061/(ASCE)0733-9445(1999)125:3(281)
Sivakamasundari, S., Daniel, A.J. and Kumar, A. (2017), "Study on flexural behavior of steel fiber RC beams confined with biaxial geo-grid", *Procedia Eng*., **173**, 1431-1438. https://doi.org/10.1016/j.proeng.2016.12.206.
Usman, M., Farooq, Syed H., Umair, M. and Hanif, A. (2020), "Axial compressive behavior of confined steel fiber reinforced high strength concrete", *Constr. Build. Mater*., **230**, 117043. https://doi.org/10.1016/j.conbuildmat.2019.117043
Zaidi, K.A., Sharma, U.K., Bhandari, N.M. and Bhargava, P. (2016), "Postheated model of confined high strength fibrous concrete", *Adv. Civil Eng*., Article ID 5659817. https://doi.org/10.1155/2016/5659817

Nomenclature

A_{sh} = area of hoop reinforcement
β = factors affecting the shape of the curve
COV = Coefficient of Variation
d_c = cross-sectional core diameter
ε_h = hoop strain
ε_{co}' = unconfined normal concrete peak strain
ε_{cf}' = the peak strain of fibrous concrete
ε_{ccf}' = peak strain of confined fiber concrete
f_{co}' = unconfined normal concrete peak stress
f_l = lateral stress
f_{le} = effective lateral stress
f_y = yield stress of hoop reinforcement
f_c' = cylindrical normal concrete stress, dimension of 150 × 300 mm at 28 days of age
f_{cf}' = cylindrical steel-fiber concrete stress, dimension of 150 × 300 mm at 28 days of age
f_{ccf}' = peak stress of confined steel-fiber concrete
k_e = confinement effectiveness coefficient
l = fiber length
d = fiber diameter
ϕ = reinforcement diameter
RI = Reinforced Index = l/d
s = Spacing of hoop
SD = Standard of Deviation
TI = Toughness Index
V_f = Volume fraction of fiber